Photon-Initiated Homolysis of Peroxynitrous Acid

ARTICLE *in* INORGANIC CHEMISTRY · JUNE 2009

Impact Factor: 4.76 · DOI: 10.1021/ic900614e · Source: PubMed

4 AUTHORS:

Manuel Sturzbecher-Hoehne
Lawrence Berkeley National Laboratory
15 PUBLICATIONS **67** CITATIONS
SEE PROFILE

Thomas Nauser
ETH Zurich
63 PUBLICATIONS **2,170** CITATIONS
SEE PROFILE

Reinhard Kissner
ETH Zurich
69 PUBLICATIONS **2,119** CITATIONS
SEE PROFILE

Willem H Koppenol
ETH Zurich
223 PUBLICATIONS **13,565** CITATIONS
SEE PROFILE

Inorganic Chemistry
Article

Inorg. Chem. **2009**, *48*, 7307–7312 **7307**
DOI: 10.1021/ic900614e

Photon-Initiated Homolysis of Peroxynitrous Acid

Manuel Sturzbecher-Höhne, Thomas Nauser, Reinhard Kissner, and Willem H. Koppenol*

Institute of Inorganic Chemistry, Department of Chemistry and Applied Biosciences, ETH Zurich, 8093 Zurich, Switzerland

Received March 30, 2009

Laser flash photolysis of ONOOH at 355 nm and a pH of 4.0−5.5 causes homolysis of ONOOH nearly exclusively at the N−O bond rather than at the O−O bond ($HO_2^{\bullet}/HO^{\bullet}$ > 25:1). All of the $NO^{\bullet}$ and $HO_2^{\bullet}$ radicals formed by photolysis subsequently recombine with a rate constant of $(1.2 \pm 0.2) \times 10^{10}$ M^{-1} s^{-1} via second-order kinetics, as demonstrated by the return of the UV/vis absorbance to initial levels. Excitation at 266 nm also yields $HO_2^{\bullet}$ and $NO^{\bullet}$, but after recombination, the absorbance levels are lower than initial values, possibly because $HO^{\bullet}$ produced by the photolysis of water reacts with ONOOH. When NO_3^-, the product of the ONOOH isomerization, is photolyzed, the $ONOO^-$ formed is rapidly protonated with a second-order rate constant of $(1.7 \pm 0.8) \times 10^{10}$ M^{-1} s^{-1}. The ONOOH decays to the starting material, NO_3^-, with a first-order rate constant of 1.2 s^{-1}. The quantum yield for the photon-initiated homolysis is 15% for both ONOOH and $ONOO^-$. We conclude that the ON−OOH and ON−OO^- bond dissociation energies are similar.

Introduction

Peroxynitrous acid, ONOOH,[1] a strong oxidant as well as a nitrating agent, may be formed in vivo[2,3] by the diffusion-limited reaction of $O_2^{\bullet -}$ and the cellular messenger $NO^{\bullet}$, $k = (1.6 \pm 0.3) \times 10^{10}$ M^{-1} s^{-1}.[4] ONOOH and $ONOO^-$ react with a variety of biomolecules[5,6] and are implicated in a variety of diseases and disorders, including atherosclerosis, inflammation, and neurodegenerative disorders.[5,7]

$ONOO^-$ is fairly stable in aqueous media at pH values above 10. In the protonated form, ONOOH decays to NO_3^- with a rate constant of 1.2 s^{-1} (reaction 1).[8] The pK_a of ONOOH is 6.5−6.8 (reaction 2), depending on the ionic strength of the solution.[8]

$$ONOOH = NO_3^- + H^+ \quad (1)$$

$$ONOOH = ONOO^- + H^+ \quad (2)$$

$$ONOO^- = NO^{\bullet} + O_2^{\bullet -} \quad (3)$$

$$ONOOH = NO_2^{\bullet} + HO^{\bullet} \quad (4)$$

$$ONOOH = NO^{\bullet} + HO_2^{\bullet} \quad (5)$$

$$HO_2^{\bullet} = O_2^{\bullet -} + H^+ \quad (6)$$

Homolysis of $ONOO^-$ at the N−O bond (reaction 3) takes place with a rate constant of 0.020 ± 0.001 s^{-1}.[9] From this rate constant and the known rate constant for reaction 3, $(1.6 \pm 0.3) \times 10^{10}$ M^{-1} s^{-1},[4] we derived standard Gibbs energies of formation of $ONOO^-$ (+68 ± 1 kJ mol^{-1}) and ONOOH

*To whom correspondence should be addressed. Phone: +41-44-632-2875. Fax +41-44-632-1090. E-mail: koppenol@inorg.chem.ethz.ch.

(1) Formulae, systematic names, and *trivial* names (in italics): $ONOO^-$, oxidoperoxidonitrate(1−), *peroxynitrite*; ONOOH, (hydridodioxido)oxidonitrogen, *peroxynitrous acid*; $O_2^{\bullet -}$, dioxide(•1−), *superoxide*; $HO_2^{\bullet}$, hydridodioxygen(•), *perhydroxyl radical or hydroperoxyl radical*; O_2, dioxygen; $O^{\bullet -}$, oxide(•1−); $NO^{\bullet}$, oxidonitrogen(•) or nitrogen monoxide, *nitric oxide*; $NO_2^{\bullet}$, dioxidonitrogen(•) or nitrogen dioxide, *pernitric oxide*; N_2O_4, tetraoxidodinitrogen, *nitrogen tetroxide*; NO_3^-, trioxidonitrate(1−), *nitrate*; $HO^{\bullet}$, hydridooxygen(•), *hydroxyl radical*; $Cl_2^{\bullet -}$, dichloride(•1−), *dichlorine radical anion*. Connelly, N. G.; Damhus, T.; Hartshorn, R. M.; Hutton, A. T. *Nomenclature of Inorganic Chemistry*. *IUPAC Recommendations 2005*; Royal Society of Chemistry: Cambridge, U.K., 2005.

(2) Beckman, J. S.; Beckman, T. W.; Chen, J.; Marshall, P. A.; Freeman, B. A. *Proc. Natl. Acad. Sci. U. S. A.* **1990**, *87*, 1620–1624.
(3) Beckman, J. S.; Koppenol, W. H. *Am. J. Physiol. Cell Physiol.* **1996**, *271*, C1424–C1437.
(4) Nauser, T.; Koppenol, W. H. *J. Phys. Chem. A* **2002**, *106*, 4084–4086.
(5) Alvarez, B.; Radi, R. *Amino Acids* **2003**, *25*, 295–311.
(6) Szabo, C.; Ischiropoulos, H.; Radi, R. *Nat. Rev. Drug Discovery* **2007**, *6*, 662–680.
(7) Pacher, P.; Beckman, J. S.; Liaudet, L. *Physiol. Rev.* **2007**, *87*, 315–424.
(8) Kissner, R.; Nauser, T.; Bugnon, P.; Lye, P. G.; Koppenol, W. H. *Chem. Res. Toxicol.* **1997**, *10*, 1285–1292.
(9) Sturzbecher, M.; Kissner, R.; Nauser, T.; Koppenol, W. H. *Inorg. Chem.* **2007**, *46*, 10655–10658.

Published on Web 06/25/2009

(+31 ± 1 kJ mol^{-1}), in excellent agreement with other published values.[10−13] We summarize the published thermodynamic values in Figure 1. The Gibbs energies of formation of ONOOH (+31 ± 1 kJ mol^{-1}),[10,12] $NO_2^•$ (63 ± 1 kJ mol^{-1}),[14] and $HO^•$ (26 ± 1 kJ mol^{-1})[15,16] and the published rate constant for reaction 4 (4.5×10^9 M^{-1} s^{-1})[17,18] have been used to predict a rate of homolysis of ONOOH at the O−O bond (reaction 4) of 0.38 ± 0.25 s^{-1}.[10,11,19] However, this approach is valid only when no branching of the reaction coordinate occurs, which is not the case here: the reaction of $HO^•$ with $NO_2^•$ yields two products, namely, ONOOH and NO_3^-/H^+.[18] Since we have searched for, but have been unable to find, evidence of significant levels of formation of $HO^•$ from ONOOH,[20−24] we attempted to stimulate reaction 4 by laser flash photolysis.

A pathway of homolysis of ONOOH, distinct from reaction 4, leads to the formation of $NO^•$ and $HO_2^•$ (reaction 5). The energies of these products of reaction lie 20 kJ mol^{-1} above those of the products of reaction 4 (Figure 1): $\Delta_f G°(NO^•) = 102 \pm 0.2$ kJ mol^{-1} is calculated from $\Delta_f G°(NO^•)g = +86.57$ kJ mol^{-1} [25] and Henry's constant, 1.92×10^{-3} M 0.100 MPa^{-1} [26] at 25 °C; $\Delta_f G°(HO_2^•) = 6.4 \pm 1.0$ kJ mol^{-1} is based on $E°(O_2/O_2^{•-}) = 350 \pm 11$ mV[27] and $pK_{a,6} = 4.8 \pm 0.1$ for $HO_2^•$.[28] With $k_{-5} = 3.2 \times 10^9$ M^{-1} s^{-1} [29] and the Gibbs energies of formation of ONOOH, $NO^•$, and $HO_2^•$, we calculate $k_5 = (0.8 \pm 1.0) \times 10^{-4}$ s^{-1}, which is more than 4 orders of magnitude lower than k_4.

We report here that $NO^•$ and $HO_2^•$, but not $NO_2^•$ and $HO^•$, are formed by the photolysis of ONOOH. The observed products recombine rapidly to form ONOOH.

Materials and Methods

Chemicals. $(Me_4N)ONOO$ was prepared from $NO^•$ and $(Me_4N)O_2$ according to the method of Bohle et al.[30−32] All reagent gases were obtained from PanGas (Dagmersellen, CH). LiONOO was prepared as previously described.[33] All other chemicals were obtained at the highest purity available and used as received. A Millipore Milli-Q unit (Molsheim, F) was used to purify deionized water.

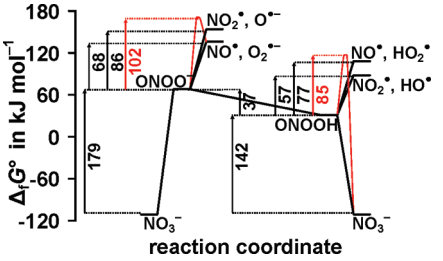

Figure 1. The reaction coordinate for the photolysis of NO_3^- showing Gibbs energies of formation of ONOOH, ONOO$^-$, and NO_3^- and possible products of homolysis and experimentally determined activation energy barriers. Activation energies and the barriers for homolysis of ONOO$^-$ to $NO^•$ and $O_2^{•-}$ and isomerization of ONOOH to NO_3^- are shown in red. Gibbs energies of reaction are shown in black.

Instrumentation. UV/vis spectra were recorded with a double-beam Analytik Jena Specord 200 (Jena, D). Rapid mixing was achieved by the stopped-flow mixing unit from Applied Photophysics, SX 17MV (Leatherhead, Surrey, Great Britain), that was operated in the symmetric mixing mode interfaced to an Applied Photophysics LKS 50 instrument (Leatherhead, Surrey, Great Britain). The quartz cell was asymmetric with a 10 mm optical path length, a 2 mm laser path length, and a total volume of 0.08 cm^3; measurements were performed at 25 °C, maintained with a thermostat. Optical changes were collected and stored on a WaveRunner 64Xi digital oscilloscope from Lecroy (Chestnut Ridge, NY). The bandwidth chosen for these experiments was 20 MHz, and the sampling rate was 200 MHz. The third ($\lambda = 355$ nm) or fourth ($\lambda = 266$ nm) harmonic of a Quantel Brilliant B Nd:YAG laser (Les Ulis Cedex, F) was used with a pulse duration of 6 ns and spot size of 9 mm. The laser energies were determined with a PRD-J peak-reading joulemeter from Gentec Inc. (Sainte-Foy, Quebec, Canada). The pH was measured with a Metrohm glass electrode (Herisau, Switzerland) interfaced with a 901 microprocessor analyzer from Orion Research, Inc. (Cambridge, MA).

Methods. Photolysis of NO_3^-. Argon-saturated 1 M NO_3^- solutions were excited at 266 nm at pH 2.9−4.4, and subsequent reactions were followed at 260 and 330 nm. Highly concentrated solutions of NO_3^- were used because of the low absorbance of NO_3^- at 266 nm ($\varepsilon_{266} = 1.5$ M^{-1} cm^{-1}). ONOO (M = $(Me_4N)^+$, Li^+) solutions were freshly prepared in 10 mM MOH (M = K^+, Li^+), kept in the dark on ice.

Photolysis of ONOO$^-$. Argon-saturated solutions of ONOO$^-$ at ca. 2 mM in 10 mM MOH were mixed by stopped-flow techniques at 25 °C with either 20 mM H_3PO_4 or 100 mM pivalate buffer as a proton source to final pH values of 2−5.5. After 5 ms of mixing, excitation of ONOOH was achieved with a laser pulse of 266 or 355 nm with energies of 10−140 mJ/pulse (266 nm) or

(10) Merényi, G.; Lind, J. *Chem. Res. Toxicol.* **1998**, *11*, 243–246.
(11) Goldstein, S.; Czapski, G.; Lind, J.; Merényi, G. *Chem. Res. Toxicol.* **2001**, *14*, 657–660.
(12) Merényi, G.; Lind, J.; Czapski, G.; Goldstein, S. *Inorg. Chem.* **2003**, *42*, 3796–3800.
(13) Lymar, S. V.; Poskrebyshev, G. A. *J. Phys. Chem. A* **2003**, *107*, 7991–7996.
(14) Stanbury, D. M. *Adv. Inorg. Chem.* **1989**, *33*, 69–138.
(15) Schwarz, H. A.; Dodson, R. W. *J. Phys. Chem.* **1984**, *88*, 3643–3647.
(16) Kläning, U. K.; Sehested, K.; Holcman, J. *J. Phys. Chem.* **1985**, *89*, 760–763.
(17) Logager, T.; Sehested, K. *J. Phys. Chem.* **1993**, *97*, 6664–6669.
(18) Merényi, G.; Lind, J.; Goldstein, S.; Czapski, G. *J. Phys. Chem. A* **1999**, *103*, 5685–5691.
(19) Lymar, S. V.; Khairutdinov, R. F.; Hurst, J. K. *Inorg. Chem.* **2003**, *42*, 5259–5266.
(20) Kissner, R.; Koppenol, W. H. *J. Am. Chem. Soc.* **2002**, *124*, 234–239.
(21) Maurer, P.; Thomas, C. F.; Kissner, R.; Rüegger, H.; Greter, O.; Röthlisberger, U.; Koppenol, W. H. *J. Phys. Chem. A* **2003**, *107*, 1763–1769.
(22) Kissner, R.; Nauser, T.; Kurz, C.; Koppenol, W. H. *IUBMB Life* **2003**, *55*, 567–572.
(23) Kissner, R.; Thomas, C.; Hamsa, M. S. A.; van Eldik, R.; Koppenol, W. H. *J. Phys. Chem. A* **2003**, *107*, 11261–11263.
(24) Kurz, C.; Zeng, X.; Hannemann, S.; Kissner, R.; Koppenol, W. H. *J. Phys. Chem. A* **2005**, *109*, 965–969.
(25) Wagman, D. D.; Evans, W. H.; Parker, V. B.; Schumm, R. H.; Halow, I.; Bailey, S. M.; Churney, K. L.; Nuttal, R. L. *J. Phys. Chem. Ref. Data* **1982**, *11*(Suppl. 2), 37–38.
(26) Wilhelm, E.; Battino, R.; Wilcock, R. J. *Chem. Rev.* **1977**, *77*, 219–262.
(27) Wardman, P. *Free Radical Res. Commun.* **1991**, *14*, 57–67.
(28) Bielski, B. H. J.; Cabelli, D. E.; Arudi, R. L. *J. Phys. Chem. Ref. Data* **1985**, *14*, 1041–1100.
(29) Goldstein, S.; Czapski, G. *Free Radical Biol. Med.* **1995**, *19*, 505–510.
(30) Bohle, D. S.; Hansert, B.; Paulson, S. C.; Smith, B. D. *J. Am. Chem. Soc.* **1994**, *116*, 7423–7424.
(31) Bohle, D. S.; Glassbrenner, P. A.; Hansert, B. *Methods Enzymol.* **1996**, *269*, 302–311.
(32) Bohle, D. S.; Sagan, E. S. *Inorg. Synth.* **2004**, *34*, 36–42.
(33) Sturzbecher-Höhne, M.; Kissner, R.; Nauser, T.; Koppenol, W. H. *Chem. Res. Toxicol.* **2008**, *21*, 2257–2259.

Table 1. Molar Absorptivities of Relevant Species, Used to Calculate Yields and Spectra in Figures 3 and 5

	Excitation λ (nm)		Observation λ (nm)		
	266, ε (M^{-1} cm^{-1})	355, ε (M^{-1} cm^{-1})	260, ε (M^{-1} cm^{-1})	330, ε (M^{-1} cm^{-1})	400, ε (M^{-1} cm^{-1})
$ONOOH$[8]	450	70	500	80	8
$ONOO^-$[8]	680	500	475	850	71
$HO^•$[45]			480		
$HO^•$[46]			430		
$HO^•$[47]			454	135	30
$HO_2^{•-}$[28,35]			540		
$O_2^{•-}$[28,35]			1940		
$NO^•$			> 10	> 10	> 10
$NO_2^•$[48]			270	150	200
N_2O_4[36,49]			750	300	

10−160 mJ/pulse (355 nm), and reactions were followed at 260, 330, and 400 nm. The pH was recorded after mixing. Transient absorbance changes at pH 4.8 were recorded by changing the wavelength settings of the monochromator in 5 nm increments from 235−300 nm. The concentration of $HO^•$, generated in photolysis experiments, was determined by mixing $ONOO^-$ in a 1:1 ratio with NaCl at different concentrations in 20 mM HCl before excitation with detection of the transient $Cl_2^{•-}$ at 340 nm (ε_{340} = 8800 M^{-1} cm^{-1} [34]); NaCl solutions photolyzed in 10 mM HCl served as controls.

Results

Photolysis of NO_3^-. We investigated the photolysis of NO_3^-, the product of isomerization of ONOOH, in the presence of the cations Li^+, Na^+, K^+, Cs^+, and $(Me_4N)^+$. We did not use $RbNO_3$, because it is not sufficiently soluble in aqueous solution. All alkali metal salts of NO_3^- behave similarly: during excitation at pH 2.9−4.4, an initial increase in absorbance at 330 nm is observed that is ascribed to the formation of $ONOO^-$, followed by a rapid decay that is linearly dependent on the H^+ concentration and represents protonation of $ONOO^-$. The protonation takes place with a second-order rate constant of $(1.7 \pm 0.8) \times 10^{10}$ M^{-1} s^{-1} (data not shown). From the absorbance of the initial product and reported absorptivities for $ONOO^-$ at 260 nm (ε = 500 M^{-1} cm^{-1}) and 330 nm (ε = 80 M^{-1} cm^{-1})[8] (Table 1), we calculated that excitation at 266 nm with a laser energy of 100 mJ/pulse results in the formation of 10 μM ONOOH. After the protonation step, we observe a first-order decay to initial absorbance levels at 260 nm with a rate constant of 1.2 s^{-1}, which we assign to the isomerization of ONOOH to NO_3^-/H^+. The behavior of $(Me_4N)NO_3$ was different from that of the alkali metal salts, with a slower increase in absorbance followed by only a single decay.

Photolysis of ONOOH. Laser flash photolysis experiments were performed with Li^+ as the counterion. LiONOO (1.76 mM) was rapidly mixed with an equal amount of 20 mM H_3PO_4 (final pH 2.1) and irradiated with laser pulses at 355 nm. Only small changes in absorbance were detected: the highest laser energy used (142 mJ/pulse) resulted in an increase of 0.004 absorbance units at 260 nm relative to the preirradiation level. Importantly, the subsequent decay in absorbance to the preirradiation absorbance level obeys second-order kinetics and is complete after 50 μs. The low signal-to-noise ratio obviated meaningful evaluation of the traces. We found larger absorbance changes at higher pH, and Figure 2a shows data collected in a 100 mM pivalate buffer at pH 4.1−5.4. The increase in absorbance at 260 nm as a function of pH approximates that expected for $HO_2^•$, the pK_a of which is 4.8 (Figure 2b).[28] When the irradiation energy is varied, a strictly linear correlation between the concentration of $HO_2^•/O_2^{•-}$ and laser energy is found (Figure 2c). Kinetics data obtained in additional experiments performed with $(Me_4N)ONOO$ were similar to those obtained with LiONOO.

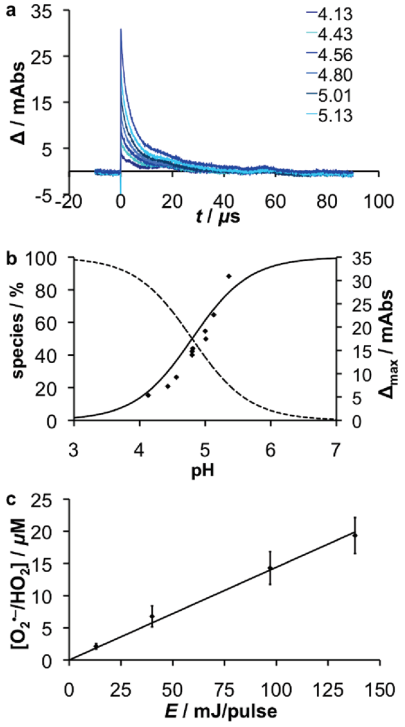

Figure 2. Photolysis (355 nm) of ONOOH, prepared by mixing 2.06 mM LiONOO in 10 mM LiOH, with a 0.1 M pivalate buffer, at pH 4.1−5.4 and 25 °C. (a) Absorbance increase at 260 nm upon irradiation and subsequent decay attributed to second-order recombination. The signal distortion at 58 μs was also observed in the absence of ONOOH. (b) Absorbance at 260 nm (red data points) measured directly after irradiation (140 mJ/pulse), with the species distributions of $HO_2^•$ (dashed line) and $O_2^{•-}$ (solid line) calculated on the basis of pK_a = 4.8. (c) Concentration of $HO_2^•/O_2^{•-}$, based on absorbance at 260 nm, as a function of laser energy.

We plotted the absorbance measured at 5 nm intervals between 235 and 300 nm after excitation (355 nm, 125 mJ/pulse) at pH 4.83 (after mixing) in Figure 3a. At pH 4.8, the concentrations of $HO_2^•$ and $O_2^{•-}$ are the same, and we used molar absorptivities from the literature[28,35] to evaluate the concentrations and rate constants to generate the calculated mixed spectrum shown in Figure 3b. That

(34) Under acidic conditions, Cl^- reacts quickly with $HO^•$ to form ultimately the strongly absorbing $Cl_2^{•-}$. This is shown in the reactions below. The yield of the transient $Cl_2^{•-}$ is dependent on the Cl^- concentration and the laser energy. $HO^• + Cl^- = HOCl^{•-}$, $HOCl^{•-} + H^+ = H_2O + Cl^•$, $Cl^• + Cl^- = Cl_2^{•-}$. Jayson, G. G.; Parsons, B. J.; Swallow, A. J. *J. Chem. Soc., Faraday Trans. 1* **1973**, *69*, 1597–1607.

(35) Bielski, B. H. J. *Photochem. Photobiol.* **1978**, *28*, 645–649.

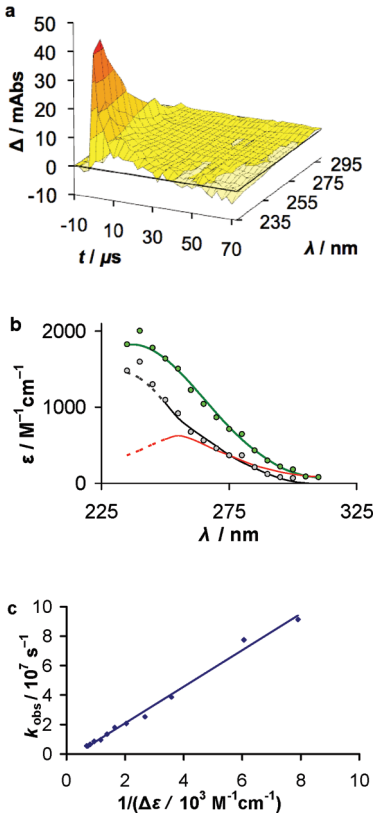

Figure 3. Spectral changes upon photolysis (355 nm, 125 mJ/pulse) of 1.1 mM $(Me_4N)ONOO$ at pH 4.8 and 25 °C, prepared from equal volumes of 2.2 mM $(Me_4N)ONOO$ in 10 mM KOH and a 0.1 M pivalate buffer. (a) Spectrum as a function of time after the pulse, showing apparent second-order decay to initial absorbance levels via recombination of $HO_2^{\bullet}/O_2^{\bullet-}$ with $NO^{\bullet}$, yield of $HO_2^{\bullet}/O_2^{\bullet-} > 25$ μM. (b) Raw spectral data (gray circles) recorded 0.07 μs after photolysis of ONOOH at pH 4.8. Spectrum of $HO_2^{\bullet}/O_2^{\bullet-}$ (green line) calculated for pH = p$K_{a,6}$ = 4.8;[28,35] experimental spectrum of ONOOH (red line), extrapolated to $\lambda < 250$ nm based on an assumed symmetric band; difference spectrum, $\Delta\varepsilon$ (gray line) = ε ($HO_2^{\bullet}/O_2^{\bullet-}$, green line) − ε (ONOOH, red line). Spectral data corrected for the bleaching of ONOOH (green points). Data points are derived from the data in a. Note that the measured absorptivities and, hence, the shape of the spectra are not dependent on the time elapsed after the flash over the range of 0.07−5 μs. The data fit a model for exclusive formation of $NO^{\bullet}$ and $HO_2^{\bullet}$ (reaction 5). (c) The observed rate constant as a function of the reciprocal effective molar absorptivity (the sum of the molar absorptivities of $HO_2^{\bullet}$, $O_2^{\bullet-}$, and ONOOH at 235−300 nm) at pH 4.8: a second-order rate constant of $(1.2 \pm 0.2) \times 10^{10}$ M^{-1} s^{-1} for the reaction of $HO_2^{\bullet}$ and $NO^{\bullet}$ to form ONOOH is determined from the slope of the line. Rate constants are derived from the data in a.

the absorbance maximum of the transient species lies near 240−245 nm is evidence for the formation of $HO_2^{\bullet}/O_2^{\bullet-}$, which indicates that irradiation causes homolysis of the N−O bond. The decay of the transient species is expected to correspond to the reaction of $HO_2^{\bullet}$ with $NO^{\bullet}$ to reform ONOOH, which should follow second-order kinetics. The concentration of $HO_2^{\bullet}/O_2^{\bullet-}$ immediately following irradiation with a laser energy of 125 mJ/pulse is >25 μM. The decay rates are plotted as a function of the reciprocal of the extinction coefficient in Figure 3c, from which we determine a second-order rate constant of $(1.2 \pm 0.2) \times 10^{10}$ $M^{-1}s^{-1}$ for reaction 5.

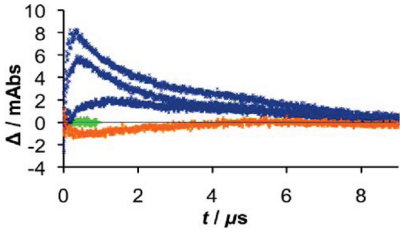

Figure 4. Trapping of $HO^{\bullet}$. Detection of $Cl_2^{\bullet-}$ at 340 nm (ε = 8800 $M^{-1}cm^{-1}$) formed in the reaction of Cl^- with $HO^{\bullet}$ in acidic solution. Solutions of 1 mM ONOOH (pH 2.1) were irradiated (355 nm, 135 mJ/pulse) in the presence of 10 mM, 60 mM, and 110 mM chloride (blue traces). The yields of $Cl_2^{\bullet-}$ increase with $[Cl^-]$ to a maximum of 0.9 μM. Control experiments: photolysis of 1.0 mM ONOOH in the absence of Cl^-, orange trace, and photolysis of 10 mM Cl^- in the absence of ONOOH, green trace.

To probe for the formation of $NO_2^{\bullet}$, we analyzed the kinetics of the reaction at 330 and 400 nm, where the absorptivity of $NO_2^{\bullet}$ and its dimer N_2O_4 is higher than that of ONOOH.[8,36] No change in absorbance was detected at 400 nm, but we observed a transient decrease in the absorbance at 330 nm that within 5 μs returned to the initial level (data not shown).

We also attempted to find evidence for the formation of $HO^{\bullet}$ during the photolysis of ONOOH, via its reaction with Cl^- under acidic conditions.[34] Solutions of NaCl at various concentrations at pH 2 (HCl) were mixed 1:1 with 2.03 mM $ONOO^-$ and irradiated. At the highest Cl^- concentration (110 mM) and a laser energy of 135 mJ/pulse, the concentration of $Cl_2^{\bullet-}$ generated from $HO^{\bullet}$ is only 0.9 μM. In the absence of Cl^-, the absorbance at 340 nm of a 1.01 mM ONOOH solution initially decreases, then returns to the initial level (Figure 4). In the absence of ONOOH, but with Cl^- present, no absorbance changes after excitation at 355 nm were observed.

We also performed photolysis of ONOOH at 266 nm (100 mJ/pulse) at pH 4.83 (after mixing) and found corroborating evidence for the formation of $HO_2^{\bullet}$ (Figure 5), followed by second-order decay. The concentration of $HO_2^{\bullet}/O_2^{\bullet-}$ after irradiation is 125 μM, much higher than that found after excitation at 355 nm, as expected since the molar absorptivity of ONOOH at 266 nm (450 M^{-1} cm^{-1}) is much higher than at 355 nm, (70 M^{-1} cm^{-1}).[8] While photolysis at 355 nm is fully reversible, that at 266 nm is not: the absorbance at 235−310 nm is significantly lower at the end of the experiment, likely due to a fast reaction of ONOOH with $HO^{\bullet}$ or $H^{\bullet}$ and e_{aq}^-, which originate from the two-photon excitation of H_2O[37,38] and, to a minor degree, by $HO^{\bullet}$ formed in reaction 4. By the irradiation of acidic Cl^- solutions, we determined that $HO^{\bullet}$ is formed in concentrations up to 5 μM.

When experiments were carried out over the wavelength range 235−300 nm, we observed for both excitation wavelengths that the rate constants increase with decreasing molar absorptivities of $HO_2^{\bullet}$ and

(36) Hug, G. L. *Optical Spectra of Nonmetallic Inorganic Transient Species in Aqueous Solution, NSRDS-NBS 69*; National Bureau of Standards: Washinton, DC, 1981.

(37) Reuther, A.; Lauberau, A.; Nikogosyan, D. N. *J. Phys. Chem.* **1996**, *100*, 16794–16800.

(38) Görner, H.; Nikogosyan, D. N. *J. Photochem. Photobiol. B: Biol.* **1997**, *39*, 84–89.

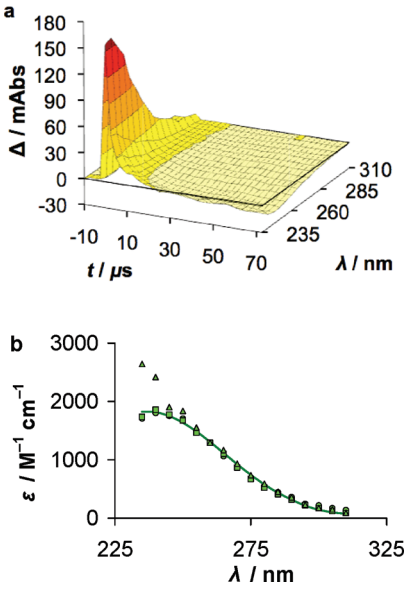

Figure 5. Spectral changes upon photolysis (266 nm, 100 mJ/pulse) of 1.1 mM $(Me_4N)ONOO$ at pH 4.8 and 25 °C, prepared from equal volumes of 2.2 mM $(Me_4N)ONOO$ in 10 mM KOH and a 0.1 M pivalate buffer. (a) Spectrum as a function of time after the pulse, showing apparent second-order decay via recombination of $HO_2^{\bullet}/O_2^{\bullet-}$ with $NO^{\bullet}$, ca. 125 μM yield of $HO_2^{\bullet}/O_2^{\bullet-}$. In contrast to photolysis at 355 nm (Figure 3a), the absorbance of the reaction mixture decays to a level lower than the initial level. (b) Spectral data, corrected for the bleaching of ONOOH, recorded at 0.07 μs (green circles) and 5 μs (green triangles) after photolysis of ONOOH at pH 4.8 and calculated spectrum of $HO_2^{\bullet}/O_2^{\bullet-}$ at pH 4.8 (green line), as in Figure 3b. Data points are derived from the data in a. In contrast to photolysis at 355 nm (Figure 3b), a systematic deviation from a model for exclusive formation of $NO^{\bullet}$ and $HO_2^{\bullet}$ (reaction 5) is observed at $\lambda > 300$ nm for 0.07 μs time points (circles) and at $\lambda < 250$ nm for 5 μs points (triangles).

$O_2^{\bullet-}$ (for excitation at 355 nm, see Figure 3c, and at 266 nm, not shown).

Quantum Yields. We irradiated solutions of 1.1 mM $ONOO^-$ in 5 mM KOH (final pH 11.7) as described by Nauser and Koppenol[4] and used eq 7 to calculate the quantum yields (ϕ) of the reactions:

$$\phi = \frac{c_{\text{products}}}{c_{\text{absorbedphotons}}} \quad (7)$$

where c_{products} is the concentration of the product; furthermore, $c_{\text{absorbed photons}} = c_{\text{totalphotons}}(1 - T)$, or

$$c_{\text{absorbedphotons}} = \frac{E_{\text{pulse}} \times \lambda}{h \times c \times N_A \times V_{\text{irradiated}}}(1 - 10^{-[\text{HOONO}] \times \varepsilon \times l_{\text{laser}}}) \quad (8)$$

where E_{pulse} is the laser energy, λ is the wavelength of irradiation, h is the Planck constant, c is the speed of light, N_A is Avogadro's number, $V_{\text{irradiated}}$ is the irradiated sample volume, ε is the molar absorptivity at the irradiation wavelength, and l_{laser} is the laser path length within the cell. The quantum yields were calculated at a delay time of 75 ns. We determined a quantum yield of 0.18 ± 0.03 for the generation of $NO^{\bullet}$ and $O_2^{\bullet-}$ from $ONOO^-$. In addition, we found the same quantum yield when we re-evaluated the experimental data in the work of Nauser and Koppenol.[4]

Similarly, we calculated a quantum yield for the induced N−O bond scission of ONOOH of 0.15 ± 0.03 at 355 m and 0.18 ± 0.04 at 266 nm. The quantum yield of the NO_3^- excitation to form ONOOH is 0.007.

Discussion

The main conclusion that we can draw from the work we present here is that laser flash photolysis of ONOOH at 355 nm causes scission of the N−O and not the O−O bond.

Photolysis of NO_3^-. Depending on pH, photolysis of the NO_3^- solutions leads to the formation of $ONOO^-$ and ONOOH.[39−44] Upon irradiation of NO_3^- solutions at 266 nm, we observe an immediate increase in absorbance, followed by a pH-dependent decay with a second-order rate constant of $(1.7 \pm 0.8) \times 10^{10}$ M^{-1} s^{-1}, which we ascribe to the protonation of $ONOO^-$ to form ONOOH, and a subsequent decay of ONOOH (k_1 = 1.2 s^{-1}).[8] Identical results were obtained for Li^+, Na^+, K^+, and Cs^+ salts of NO_3^-; $RbNO_3$ could not be tested because of its low solubility. Photolysis of $(Me_4N)NO_3$ solutions yields qualitatively different results, in which we observe an initial absorbance increase instead of a rapid decay that we assume is due to the reaction of $(Me_4N)^+$ with products of two-photon processes. It is possible that irradiation of solutions at 266 nm results in a two-photon excitation of H_2O to generate reactive species such as $HO^{\bullet}$. Since alkali metal ions, unlike $(Me_4N)^+$, do not react with $HO^{\bullet}$, we decided to use LiONOO for experiments with ONOOH.

Photolysis of ONOOH. At pH 2.1, with excitation at 355 nm, the photolysis of ONOOH triggers a *reversible* process: We observe an increase in absorbance at 260 nm upon photolysis that is pH-dependent between pH 4.1 and 5.4 (Figure 2B), as well as bleaching at 330 nm, both of which return to preirradiation levels. The increase in absorption at 260 nm could be explained by the formation of either $NO_2^{\bullet}$ + $HO^{\bullet}$ (reaction 4) or $HO_2^{\bullet}$ + $NO^{\bullet}$ (reaction 5). However, we favor the reversible formation of $HO_2^{\bullet}$ and $NO^{\bullet}$ (reaction 5) over reaction 4 as the major pathway, because (i) at 260 nm, we observe a pH-dependent increase in absorbance around pH = 4.8, the $pK_{a,6}$ of $HO_2^{\bullet}$ (Figure 2B),[28] whereas the sum of absorptivities of $HO^{\bullet}$ and $NO_2^{\bullet}$ is not pH-dependent, as neither $NO_2^{\bullet}$ nor $HO^{\bullet}$ has a pK_a in that region at 260 nm; (ii) the bleaching observed at 330−400 nm, rather than the absorption increase expected for reaction 4, may be explained by the formation of $HO_2^{\bullet}$ and $NO^{\bullet}$ (reaction 5), because the molar absorbtivities of $HO_2^{\bullet}$ and $NO^{\bullet}$ at 330 nm are lower than that of ONOOH (Table 1); (iii) the scavenging experiments with Cl^- indicate that $^{\bullet}OH$ formation is negligible, and neither $HO_2^{\bullet}$ nor $NO^{\bullet}$ would oxidize Cl^-; (iv) any excess ONOOH is expected to be oxidized by $^{\bullet}OH$ but not by $HO_2^{\bullet}$ or $NO^{\bullet}$; thus, the relaxation of the absorbance signal for ONOOH to the preirradiation level indicates that no $^{\bullet}OH$ is formed (by contrast, $^{\bullet}OH$ from the radiolysis of water produced by irradiation at 266 nm reacts with excess ONOOH, and

(39) Papée, H. M.; Petriconi, G. L. *Nature* **1964**, *204*, 142–144.
(40) Shuali, U.; Ottolenghi, M.; Rabani, J.; Yelin, S. *J. Phys. Chem.* **1969**, *73*, 3445–3451.
(41) Barat, F.; Gilles, L.; Hickel, B.; Sutton, J. *J. Chem. Soc. A* **1970**, 1982–1986.
(42) Bayliss, N. S.; Bucat, R. B. *Aust. J. Chem.* **1975**, *28*, 1865–1878.
(43) Wagner, I.; Strehlow, H.; Busse, G. *Z. Physik. Chem.* **1980**, *123*, 1–33.
(44) Madsen, D.; Larsen, J.; Jensen, S. K.; Keiding, S. R.; Thøgersen, J. *J. Am. Chem. Soc.* **2003**, *125*, 15571–15576.

relaxation of the absorbance signal to preirradiation levels is not observed); and (v) at both excitation wavelengths, the spectra collected at pH 4.83 fit calculated spectra.

We report here a rate constant $k_{-5} = (1.2 \pm 0.2) \times 10^{10}$ M^{-1} s^{-1} for the recombination of $HO_2^{\bullet}$ with $NO^{\bullet}$ at pH 4.1−5.4. This rate constant is ca. 4-fold higher than the value obtained by pulse radiolysis, 3.2×10^9 M^{-1} s^{-1},[29] and equivalent to that observed in basic aqueous solutions for the reaction of $O_2^{\bullet-}$ with $NO^{\bullet}$, $(1.6 \pm 0.3) \times 10^{10}$ M^{-1} s^{-1}.[4] With $k_{-5} = (1.2 \pm 0.2) \times 10^{10}$ M^{-1} s^{-1}, we calculate a rate constant $k_5 = 0.0003$ s^{-1} for the homolysis of ONOOH to $HO_2^{\bullet}$ and $NO^{\bullet}$. This rate constant indicates that it is not possible to detect this homolysis reaction because ONOOH isomerizes with a rate constant of 1.2 s^{-1}.

The results of our investigations of photolysis of $(Me_4N)ONOO$ solutions (Figure 3) were similar to those found with LiONOO (Figure 2), probably because the concentration of $(Me_4N)ONOO$ was much lower, 1 mM, than the 1 M solutions used in the $(Me_4N)NO_3$ experiments. The decay in absorbance after photolysis at 266 nm of $(Me_4N)ONOO$ solutions ends at levels lower than the absorbance of the initial mixture (Figure 5), possibly because two-photon processes lead to the formation of products that react either with the remaining ONOOH or with the formed $HO_2^{\bullet}$, $O_2^{\bullet-}$, and $NO^{\bullet}$. We further assume that $HO^{\bullet}$ produced by two-photon excitation of H_2O reacts more rapidly with ONOOH than with $(Me_4N)^+$.

Quantum Yields. For all experimental conditions, whether acidic (ONOOH) or basic ($ONOO^-$), the quantum yields resulting from excitation at 266 or 355 nm are essentially identical (15%) within the error, which allows us to conclude that similar energies are required to break the N−O bond in both $ONOO^-$ and ONOOH. The activation energy for homolysis of the N−O bond of $ONOO^-$ is 102 kJ mol^{-1} and that of O_2NOO^- is 93 kJ mol^{-1};[9,50] hence, we estimate a N−O bond dissociation energy of 100 kJ mol^{-1} for ONOOH. Furthermore, we assume that the remaining 85% of the quantum yield can be assigned to an excited state of ONOOH that rapidly decays to the ground state.

Formation of $HO^{\bullet}$ by Photolysis. To detect yields of O−O homolysis, we trapped $HO^{\bullet}$ with Cl^-. In contrast to Br^- and I^-, Cl^- does not react with ONOOH or its decomposition products.[24,51,52] We determined a yield of 0.9 μM $HO^{\bullet}$ for the homolysis of ONOOH under conditions that produced more than 25 μM HO_2 and $NO^{\bullet}$. In control experiments in which we irradiated acidic Cl^- solutions at 355 nm laser light (135 mJ/pulse) in the absence of ONOOH, we observed no formation of $Cl_2^{\bullet-}$ at 340 nm. However, with excitation at 266 nm (108 mJ/pulse), we observed the formation of 5 μM $HO^{\bullet}$, which implies that two-photon reactions are relevant at this excitation wavelength.[37] Subsequent reaction of $HO^{\bullet}$ with ONOOH explains the loss of absorbance after the recombination of $HO_2^{\bullet}$ and $NO^{\bullet}$. We assume that the rate constant for the reaction of $HO^{\bullet}$ with concentrated ONOOH is similar to that for the reaction with the anion, $(4.8-5.8) \times 10^9$ M^{-1} s^{-1}.[8,53] By implication, then, two-photon excitation of the solvent at 355 nm is irrelevant, and any $Cl_2^{\bullet-}$ formed originates from the $HO^{\bullet}$ generated by ONOOH photolysis. The reaction of $O_2^{\bullet-}$ with Cl^- is negligible, with a rate constant of < 0.014 M^{-1} s^{-1}.[54] Reactions of $HO_2^{\bullet}$ and $O_2^{\bullet-}$ with $HO^{\bullet}$, which have rate constants of $(0.7-1.0) \times 10^{10}$ $M^{-1}s^{-1}$,[55,56] and $(0.9-1.0) \times 10^{10}$ $M^{-1}s^{-1}$,[55,56] respectively, and of $NO^{\bullet}$ with $HO^{\bullet}$, with a rate constant of $(1.7-2.0) \times 10^{10}$ M^{-1} s^{-1},[49,57] are also unimportant. Finally, with respect to the reaction of $NO^{\bullet}$ with $HO_2^{\bullet}$, we can neglect reactions of $HO_2^{\bullet}$ with itself ($k = 1.0 \times 10^6$ M^{-1} s^{-1})[58] or with $O_2^{\bullet-}$ ($k = 9.7 \times 10^7$ M^{-1} s^{-1}).[28]

Our results obtained by photolysis at 355 nm show that the yields of the photolysis products are < 5% of $HO^{\bullet}$ and $NO_2^{\bullet}$ in comparison to > 95% of $HO_2^{\bullet}$ and $NO^{\bullet}$. These results are counterintuitive within the framework of the given thermodynamic data on ONOOH, $NO^{\bullet}$, $HO_2^{\bullet}$, $NO_2^{\bullet}$, and $HO^{\bullet}$ shown in Figure 1 in that, without regard to activation energies, these data favor $NO_2^{\bullet}$ and $HO^{\bullet}$ as homolysis products. An obvious argument is that photochemistry processes involve excited states and reaction pathways different from those that involve ground-state structures.

In a report combining infrared spectroscopy data with quantum calculations, it has been suggested that ONOOH may undergo homolysis, directly and reversibly, to form $NO^{\bullet}$ and $HO_2^{\bullet}$, and, indirectly, by way of several intermediates to $NO_2^{\bullet}$ and $HO^{\bullet}$.[59] Additionally, isomerization to NO_3^- and H^+ acts as a sink that effectively prevents the formation of free $NO_2^{\bullet}$ and $HO^{\bullet}$. If this is so, then how can ONOOH act as a powerful oxidant? According to a recent ab initio study, ONOOH reacts by way of a two-state reactivity paradigm in which the activated and oxidizing form of ONOOH is a triplet-state intermediate described as a "hydroxyl radical stabilized by a nitrogen dioxide group".[60] The findings of Contreras et al.[60] support our position that isomerization of ONOOH takes place via intramolecular reorganization rather than by homolysis.

Acknowledgment. We thank Dr. P. L. Bounds for helpful discussions and linguistic advice. The studies were supported by the ETH Zurich and the Swiss National Science Foundation.

(45) Nielsen, S. O.; Michael, B. D.; Hart, E. J. *J. Phys. Chem.* **1976**, *80*, 2482–2488.
(46) Pagsberg, P.; Christensen, H.; Rabani, J.; Nilsson, G.; Fenger, J.; Nielsen, S. O. *J. Phys. Chem.* **1969**, *73*, 1029–1038.
(47) Czapski, G.; Bielski, B. H. J. *Radiat. Phys. Chem.* **1993**, *41*, 503–505.
(48) Grätzel, M.; Henglein, A.; Lilie, J.; Beck, G. *Ber. Bunsenges. Physik. Chem.* **1969**, *73*, 646–653.
(49) Treinin, A.; Hayon, E. *J. Am. Chem. Soc.* **1970**, *92*, 5821–5828.
(50) Zabel, F. *Z. Physik. Chem.* **1995**, *188*, 119–142.
(51) Halfpenny, E.; Robinson, P. L. *J. Chem. Soc.* **1952**, 928–938.
(52) Goldstein, S.; Czapski, G. *Inorg. Chem.* **1995**, *34*, 4041–4048.
(53) Goldstein, S.; Saha, A.; Lymar, S. V.; Czapski, G. *J. Am. Chem. Soc.* **1998**, *120*, 5549–5554.
(54) Long, C. A.; Bielski, B. H. J. *J. Phys. Chem.* **1980**, *84*, 555–557.
(55) Sehested, K.; Rasmussen, O. L.; Fricke, H. *J. Phys. Chem.* **1968**, *72*, 626–630.
(56) Elliot, A. J.; Buxton, G. V. *J. Chem. Soc., Faraday Trans.* **1992**, *88*, 2465–2470.
(57) Strehlow, H.; Wagner, I. *Z. Phys. Chem.* **1982**, *132*, 151–160.
(58) Christensen, H.; Sehested, K. *J. Phys. Chem.* **1988**, *92*, 3007–3011.
(59) Konen, I. M.; Pollack, I. B.; Li, E. X. J.; Lester, M. I.; Varner, M. E.; Stanton, J. F. *J. Chem. Phys.* **2005**, *122*, 094320−1–094320−16.
(60) Contreras, R.; Galván, M.; Oliva, M.; Safont, V. S.; Andrés, J.; Guerra, D.; Aizman, A. *Chem. Phys. Lett.* **2008**, *457*, 216–221.